

Reflectarray Design for Satellite Applications with Very Low Cross-Polarization Requirements

Daniel R. Prado*, Manuel Arrebola†, George Goussetis*

*Institute of Sensors, Signals and Systems, Heriot-Watt University, Edinburgh, U.K. Email: {dr38, g.goussetis}@hw.ac.uk

†Group of Signal Theory and Communications, Universidad de Oviedo, Spain. Email: arrebola@uniovi.es

Abstract—Modern satellite applications for communications require a high polarization purity, usually with parameters such as the crosspolar discrimination (XPD) larger than 33 dB. To achieve these values, some form of cross-polarization performance optimization must be carried out. The usual approach is to minimize the crosspolar component of the far field with regard to the copolar pattern in the region of interest. However, this generates suboptimal results since the figure of merit for cross-polarization performance, i.e. the XPD, is optimized indirectly. Thus, it is proposed to directly optimize the figure of merit to considerably improve the polarization purity of reflectarray antennas for satellite applications. For that purpose, the generalized Intersection Approach algorithm is used in a large reflectarray for a contoured beam application with European coverage. It is shown that directly optimizing the cross-polarization figure of merit provides better results than the usual approach of minimizing the crosspolar pattern.

Index Terms—Reflectarray, satellite applications, polarization purity, crosspolar discrimination, crosspolar isolation, cross-polarization performance, contoured beam

I. INTRODUCTION

Cross-polarization performance is a parameter of interest in satellite applications [1], and in particular a number of strategies have been proposed in the past years to minimize the crosspolar pattern of reflectarray antennas. The first approaches dealt with a proper arrangement of the unit cells [2], [3], looking for symmetries in order to cancel the contribution of the reflectarray elements to the crosspolar pattern. Another approach was to directly minimize the cross-polarization introduced by each reflectarray element, minimizing the undesired tangential field [4], [5]. The main advantage of these techniques that work at the element level is that they are relatively fast. However the crosspolar pattern is minimized indirectly and the techniques are limited in scope and provide suboptimal results.

A more flexible approach, albeit computationally slower, is to work at the radiation pattern level, directly minimizing the crosspolar far field through a cost function. The first attempts at directly optimizing the reflectarray geometry were done with a full-wave technique based on local periodicity (FW-LP) [6], but it was slow, only dealt with one polarization and small reflectarrays. Later, some computational techniques were introduced that allow to optimize very large reflectarrays with a FW-LP and handle thousands of optimizing variables with success [7]. A faster approach for the direct optimization of reflectarrays is the use of databases instead of a FW-LP tool, since computations are considerably accelerated [8].

All these approaches have in common that the cost function minimizes the crosspolar component of the far field, so that parameters of interest such as the crosspolar discrimination (XPD) or crosspolar isolation (XPI) are improved indirectly, thus providing again suboptimal results.

In this work it is proposed to directly optimize the XPD or XPI parameters in the cost function. In this way, the cross-polarization performance of the final reflectarray antenna will improve. It will be shown how this strategy provides better results than to directly minimize the crosspolar pattern. For this task, the generalized Intersection Approach algorithm is chosen to optimize a large reflectarray for Direct Broadcast Satellite (DBS) service as an example of application. However, the technique is general and may be employed for other applications such as Synthetic Radar Aperture (SAR) [9] or multibeam [10], where cross-polarization performance is also important.

II. ANTENNA DESIGN

A. Antenna Specifications

A sketch of the antenna geometry under study is presented in Fig. 1. The reflectarray is elliptical with a total of 4068 elements distributed in a regular grid with 74 and 70 unit cells in the main axes. The periodicity is $14\text{ mm} \times 14\text{ mm}$, which is 0.553λ at the working frequency of 11.85 GHz. The feed is modelled with a $\cos^q \theta$ function with $q = 23$, which imposes an illumination taper of -17.9 dB at the reflectarray edges. In addition, the feed is at $\vec{r}_f = (-358, 0, 1070)\text{ mm}$ with regard to the center of the reflectarray. The antenna is placed on a satellite in geostationary orbit at 10° E longitude. Regarding the substrate of the unit cell, the bottom layer has a height of $h_A = 2.363\text{ mm}$ and a complex relative permittivity $\epsilon_{r,A} = 2.55 - j2.295 \cdot 10^{-3}$, while the top layer has a height of $h_B = 1.524\text{ mm}$ and a complex relative permittivity $\epsilon_{r,B} = 2.17 - j1.953 \cdot 10^{-3}$ (see Fig. 1).

The copolar requirements for both linear polarizations are shown in Fig. 2. A European footprint with two distinct coverages zones has been chosen, each with a different copolar gain requirement as shown in Fig. 2. The outer contours for each zone represent the specifications taking into account typical satellite pointing errors (0.1° in roll and pitch, 0.5° in yaw). The optimization will be carried out using the outer contours in the specification masks.

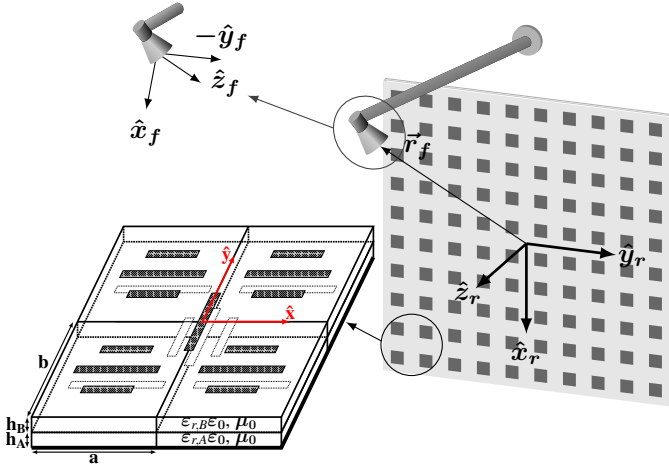


Fig. 1. Diagram of the single-offset reflectarray configuration considered in this work and the employed unit cell for dual-linear polarization applications.

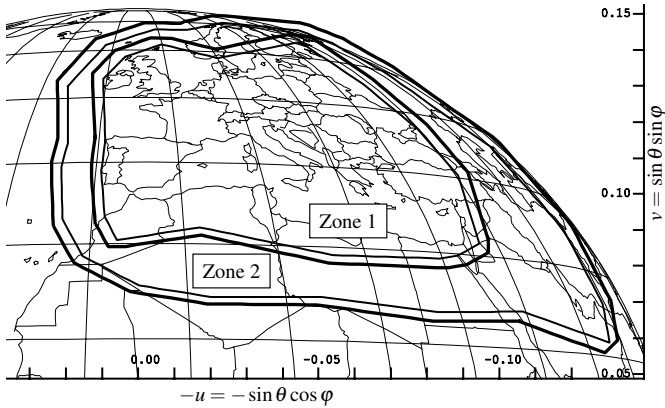


Fig. 2. European footprint with two coverage zones. The copolar requirements are 28.5 dBi and 25.2 dBi for Zones 1 and 2, respectively, and both linear polarizations.

B. The Generalized Intersection Approach

In the present case, the generalized Intersection Approach (IA) [11] has been chosen as optimization algorithm. Specifically, the particularization for reflectarray direct optimization described in [7] is used. It is an iterative algorithm that performs two operations on the radiated field at each iteration:

$$\vec{E}_{i+1} = \mathcal{B} \left[\mathcal{F} \left(\vec{E}_i \right) \right], \quad (1)$$

where \mathcal{F} is the forward projector, which computes the radiated field and then trims it according to some specifications given in the form of lower and upper masks; and \mathcal{B} is the backward projector, which minimizes the distance between the current radiated field by the reflectarray and the field trimmed by the forward projector that complies with the specifications [7].

The forward projector imposes the requirements of the far field by means of masks for the copolar and crosspolar patterns. In this way, following the notation in [7], the radiation pattern should fulfil the following condition:

$$T_{cp,\min}(u, v) \leq G_{cp}(u, v) \leq T_{cp,\max}(u, v), \quad (2a)$$

$$T_{xp,\min}(u, v) \leq G_{xp}(u, v) \leq T_{xp,\max}(u, v), \quad (2b)$$

where T_{\min} and T_{\max} denote the minimum and maximum mask specifications, respectively; and G_{cp} and G_{xp} are the radiation pattern in gain for the copolar and crosspolar components, respectively. Using the conditions in (2), the crosspolar pattern is minimized and thus the XPD and XPI are optimized indirectly. Thus, in this work it is proposed to substitute the condition (2b) by another condition which takes into account the figure of merit of interest for cross-polarization, either the XPD or the XPI, while the condition in (2a) is left untouched to guarantee that copolar requirements are also met.

C. Copolar Design

Before actually carrying out the optimization of the cross-polarization parameters, a phase-only synthesis (POS) in dual-linear polarization is performed in order to obtain a good starting point for the crosspolar optimization. Thus, the followed approach is a two-step procedure. The POS follows [12] and gives a phase-shift that each reflectarray element must provide in order to radiate the desired copolar pattern. Then, the layout is obtained using a zero-finding routine [13], adjusting the lengths of the dipoles shown in Fig. 1. Fig. 3 shows the initial radiation pattern for polarization X. As it can be seen, the copolar pattern perfectly complies with the requirements in the two coverage zones. Similar results were obtained for polarization Y. Regarding the cross-polarization performance for Zone 1, the XPD_{\min} is 31.46 dB and the XPI is 30.13 dB, the same for both linear polarizations. For Zone 2, the XPD_{\min} is 27.98 dB and 28.45 dB for polarizations X and Y, respectively; while the XPI is 25.92 dB and 26.44 dB for polarizations X and Y, respectively.

D. Optimization of XPD and XPI

For the purpose of the cross-polarization performance optimization, the XPD and XPI are considered in linear scale. Thus, the XPD is defined as the ratio, point by point, of the copolar gain and the crosspolar gain:

$$XPD(u, v) = \frac{G_{cp}(u, v)}{G_{xp}(u, v)}, \quad \forall (u, v) \in \Omega, \quad (3)$$

where Ω is a subset of the visible region ($u^2 + v^2 < 1$) corresponding to one or several coverage zones where the XPD is considered. The performance of the XPD is constrained by its minimum value, which will be the one considered in the optimization:

$$XPD_{\min} = \min \{ XPD(u, v) \}. \quad (4)$$

Similarly, the XPI is defined as the ratio between the minimum copolar gain and the maximum crosspolar gain for the coverage zone:

$$XPI = \frac{\min \{ G_{cp}(u, v) \}}{\max \{ G_{xp}(u, v) \}}, \quad (u, v) \in \Omega. \quad (5)$$

Taking into account the definition of XPD_{\min} and XPI, the goal of the optimization is to maximize their values. Thus,

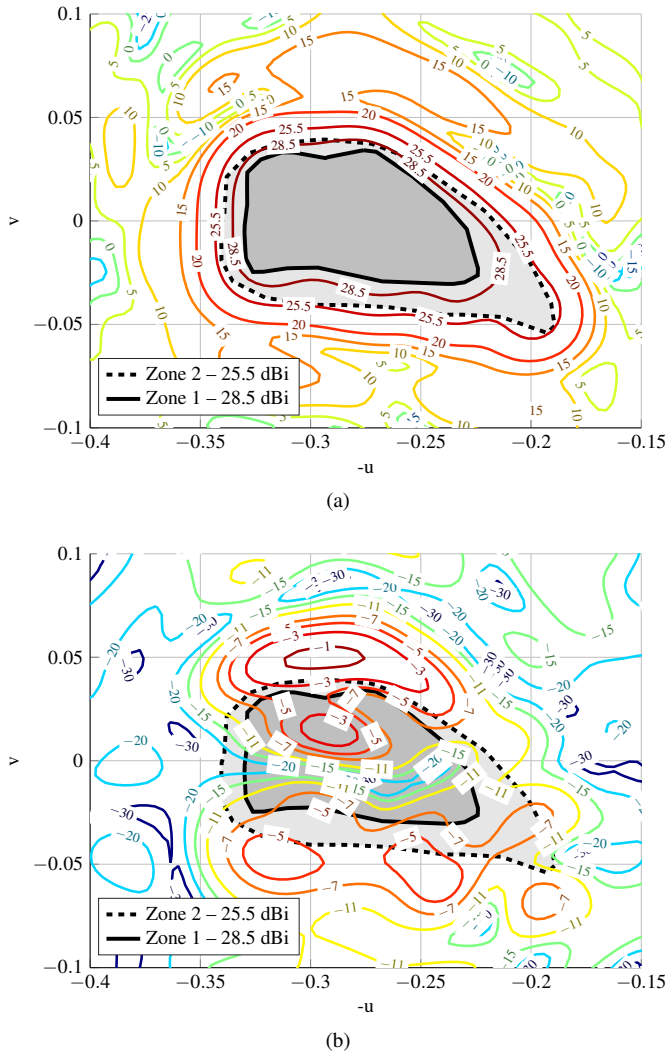


Fig. 3. Far field in dBi for polarization X of the starting point before the cross-polarization improvement obtained with POS. (a) Copolar. (b) Crosspolar.

only minimum mask specifications are necessary, fulfilling the following conditions:

$$T_{\text{XPD}_{\min}, \min} \leq \text{XPD}_{\min}, \quad (6a)$$

$$T_{\text{XPI}, \min} \leq \text{XPI}. \quad (6b)$$

Thus, condition (2b) in the forward projector is substituted by either (6a) or (6b), depending on the parameter that will be optimized.

E. Crosspolar Optimization Results

To test the proposed approach, three different optimizations will be carried out. The first one consists in minimizing the crosspolar pattern as is usual, using the condition (2b) in the forward projector. In this case, the template is set 40 dB below the maximum copolar gain to reduce the crosspolar pattern as much as possible. The second optimization uses (6a) to maximize the XPD_{\min} , and the template is also set to 40 dB. Finally, the third optimization uses the condition (6b), setting the template to 40 dB to directly improve the XPI. For all

these optimizations, the starting point is the same (shown in Fig. 3), and the copolar template specified by means of (2a) is also considered, in order to maintain the copolar gain within specifications while the cross-polarization performance is improved.

Table I shows the results for the three optimizations including the starting point as reference. In all cases, the minimum copolar gain in both coverage zones for both linear polarizations complies with the requirements of 28.5 dB for Zone 1 and 25.5 dB for Zone 2. In addition, the cross-polarization performance was greatly improved. The first optimization strategy (XP opt., i.e. minimize the crosspolar far field) improves the XPD_{\min} and XPI between 3.18 dB and 5.19 dB. The largest improvement is for the XPI in Zone 2, since the starting point presented a very low XPI. In this case, the XPI is improved 5.19 dB in polarization X and 4.63 dB in polarization Y.

When directly optimizing the XPD_{\min} , the achieved results are considerably better. In this case, the improvement in XPD_{\min} and XPI for both coverage zones and polarizations range between 7.33 dB and 8.31 dB, which contrasts with the previous case where the improvements were lower. Since the XPD_{\min} is the optimization parameter, its improvement is better than the XPI, as shown in Table I. In addition, due to the definitions in (4) and (5), the XPI is a stricter parameter than the XPD_{\min} , and the XPI will be always lower or equal than the XPD_{\min} , regardless of the parameter which is object of the optimization. Finally, optimizing the XPI improves the results of the XPI parameter with regard to the previous case, while keeping the overall improvement of the cross-polarization performance higher than when minimizing the crosspolar pattern.

Finally, Table II summarizes the improvement in cross-polarization performance for the three optimization strategies with regard to the starting point.

III. CONCLUSION

This work has proposed the direct optimization of the figure of merit of cross-polarization to improve the performance of the final antenna. The usual approach consists in the minimization of the crosspolar component of the far field, so parameters such as the crosspolar discrimination (XPD) or crosspolar isolation (XPI) are optimized indirectly. Thus, in this work the direct optimization of the XPD and XPI has been addressed to improve the cross-polarization performance of reflectarrays for space applications. The chosen algorithm is the generalized Intersection Approach, where the copolar and crosspolar requirements are specified as minimum and maximum masks. Thus, by properly setting minimum masks attending to the definition of XPD_{\min} and XPI, those parameters can be effectively optimized. As an example, a large reflectarray for Direct Broadcast Satellite application has been considered with a European footprint with two different coverage zones. As an starting point, a layout obtained after a phase-only synthesis is employed. Then, the geometry of the reflectarray was directly optimized following three different strategies: first, minimizing the crosspolar pattern,

Table I

RESULTS OF THE DIRECT OPTIMIZATION OF A REFLECTARRAY ANTENNA WITH A EUROPEAN FOOTPRINT WITH TWO COVERAGE ZONES COMPARING DIFFERENT STRATEGIES: THE USUAL APPROACH OF MINIMIZING THE CROSSPOLAR COMPONENT OF THE RADIATION PATTERN (XP OPT.) AND THE NEW STRATEGY OF DIRECTLY OPTIMIZING THE FIGURE OF MERIT (XPD_{MIN} OPT. AND XPI OPT.). CP_{MIN} IS IN DBI, XPD_{MIN} AND XPI ARE IN DB.

	Zone 1 (28.5 dBi)						Zone 2 (25.5 dBi)					
	Pol. X			Pol. Y			Pol. X			Pol. Y		
	CP _{min}	XPD _{min}	XPI									
Initial	29.29	31.46	30.13	29.32	31.46	30.13	26.03	27.98	25.92	26.03	28.45	26.44
XP opt.	29.30	35.10	34.57	29.26	35.60	33.38	26.27	31.85	31.11	26.31	31.63	31.07
XPD_{min} opt.	29.00	39.64	37.46	29.08	39.36	37.46	25.96	35.96	33.46	25.67	36.76	33.81
XPI opt.	29.04	39.53	39.25	29.01	40.32	39.00	25.80	34.78	34.49	26.06	36.29	35.75

Table II

IMPROVEMENT IN DB OF THE CROSS-POLARIZATION PERFORMANCE OF THE THREE OPTIMIZATION APPROACHES WITH REGARD TO THE STARTING POINT, WITH REFERENCE TO THE RESULTS OF TABLE I.

	Zone 1 (28.5 dBi)				Zone 2 (25.5 dBi)			
	Pol. X		Pol. Y		Pol. X		Pol. Y	
	XPD _{min}	XPI						
XP opt.	3.64	4.44	4.14	3.25	3.87	5.19	3.18	4.63
XPD_{min} opt.	8.18	7.33	7.90	7.33	7.98	7.54	8.31	7.37
XPI opt.	8.07	9.12	8.86	8.87	6.80	8.57	7.84	9.31

second maximizing the XPD_{min} and third maximizing the XPI. The results show that all three strategies improve the cross-polarization performance while keeping the copolar pattern within requirements. However, the new proposed approach of directly improving the XPD_{min} or XPI provides results that are 3 dB to 5 dB better than when minimizing the crosspolar pattern. This means that the improvement over the starting point is better than 7 dB, and reaches an improvement in the XPI of more than 9 dB. Finally, the proposed strategy may be applied to circular polarized reflectarrays as well as to the optimization over a certain bandwidth.

ACKNOWLEDGMENT

This work was supported in part by the European Space Agency (ESA) under contract ESTEC/AO/1-7064/12/NL/MH; by the Ministerio de Ciencia, Innovación y Universidades under project TEC2017-86619-R (ARTEINE); by the Ministerio de Economía, Industria y Competitividad under project TEC2016-75103-C2-1-R (MYRADA); and by the Gobierno del Principado de Asturias through Programa "Clarín" de Ayudas Postdoctorales / Marie Curie-Cofund under project ACA17-09.

REFERENCES

- [1] W. A. Imbriale, S. Gao, and L. Boccia, Eds., *Space Antenna Handbook*. Hoboken, NJ, USA: John Wiley & Sons, 2012.
- [2] D.-C. Chang and M.-C. Huang, "Multiple-polarization microstrip reflectarray antenna with high efficiency and low cross-polarization," *IEEE Trans. Antennas Propag.*, vol. 43, no. 8, pp. 829–834, Aug. 1995.
- [3] H. Hasani, M. Kamyab, and M. Ali, "Low cross-polarization reflectarray antenna," *IEEE Trans. Antennas Propag.*, vol. 59, no. 5, pp. 1752–1756, May 2011.
- [4] C. Tienda, J. A. Encinar, M. Arrebola, M. Barba, and E. Carrasco, "Design, manufacturing and test of a dual-reflectarray antenna with improved bandwidth and reduced cross-polarization," *IEEE Trans. Antennas Propag.*, vol. 61, no. 3, pp. 1180–1190, Mar. 2013.
- [5] R. Florencio, J. A. Encinar, R. R. Boix, G. Pérez-Palomino, and G. Toso, "Cross-polar reduction in reflectarray antennas by means of element rotation," in *10th European Conference on Antennas and Propagation (EuCAP)*, Davos, Switzerland, Apr. 10–15, 2016, pp. 1–5.
- [6] O. M. Bucci, A. Capozzoli, G. D'Elia, and S. Musto, "A new approach to the power pattern synthesis of reflectarrays," in *Proc. URSI International Symposium on Electromagnetic Theory (EMTS'04)*, Pisa, Italy, May 23–27, 2004, pp. 1053–1055.
- [7] D. R. Prado, M. Arrebola, M. R. Pino, R. Florencio, R. R. Boix, J. A. Encinar, and F. Las-Heras, "Efficient crosspolar optimization of shaped-beam dual-polarized reflectarrays using full-wave analysis for the antenna element characterization," *IEEE Trans. Antennas Propag.*, vol. 65, no. 2, pp. 623–635, Feb. 2017.
- [8] M. Zhou, S. B. Sørensen, O. S. Kim, E. Jørgensen, P. Meincke, and O. Breinbjerg, "Direct optimization of printed reflectarrays for contoured beam satellite antenna applications," *IEEE Trans. Antennas Propag.*, vol. 61, no. 4, pp. 1995–2004, Apr. 2013.
- [9] C. Tienda, M. Younis, P. López-Dekker, and P. Laskowski, "Ka-band reflectarray antenna system for SAR applications," in *The 8th European Conference on Antennas and Propagation (EuCAP)*, The Hague, The Netherlands, Apr. 6–11, 2014, pp. 1603–1606.
- [10] E. Martínez-de-Rioja, J. A. Encinar, A. Pino, B. González-Valdés, S. V. Hum, and C. Tienda, "Bifocal design procedure for dual reflectarray antennas in offset configurations," *IEEE Antennas Wireless Propag. Lett.*, vol. 17, no. 8, pp. 1421–1425, Aug. 2018.
- [11] O. M. Bucci, G. D'Elia, G. Mazzarella, and G. Panariello, "Antenna pattern synthesis: a new general approach," *Proc. IEEE*, vol. 82, no. 3, pp. 358–371, Mar. 1994.
- [12] D. R. Prado, M. Arrebola, M. R. Pino, and F. Las-Heras, "Improved reflectarray phase-only synthesis using the generalized intersection approach with dielectric frame and first principle of equivalence," *Int. J. Antennas Propag.*, vol. 2017, pp. 1–11, May 2017.
- [13] J. Huang and J. A. Encinar, *Reflectarray Antennas*. Hoboken, NJ, USA: John Wiley & Sons, 2008.